Synthesis and Lithium Insertion into Nanophase $MgTi_2O_5$ with Pseudo-Brookite Structure

M. Anji Reddy,[†] M. Satya Kishore,[‡] V. Pralong,[‡] V. Caignaert,[‡] U. Venkata Varadaraju,*[,†] and B. Raveau[‡]

Materials Science Research Centre and Department of Chemistry, Indian Institute of Technology Madras, Chennai 600 036, India, and Laboratoire CRISMAT, CNRS ENSICAEN, 6 bd Maréchal Juin, 14050 CAEN Cedex, France

Received October 1, 2007. Revised Manuscript Received January 7, 2008

Micrometer-sized and nanometer-sized samples of $MgTi_2O_5$ were prepared by solid state reaction and polymerizable complex methods. Electrochemical lithium insertion was studied for the first time. We observe a remarkable change in the material response when particle size is reduced from micrometer to nanometer regime. In micrometer sized samples, 0.8 Li per formula unit could be inserted, and no reversible extraction of lithium is observed. In case of nanometer-sized samples, 2.1Li are inserted and 1Li can be reversibly extracted even after 50 cycles. In the case of nanometer sized samples, formation of a new phase with approximate composition $Li_2MgTi_2O_5$ is evident form ex situ XRD studies. HRTEM studies reveal that the new phase can be considered as a distorted analogue of the parent phase.

Introduction

There is growing evidence that solid state materials behave differently with regard to lithium insertion/extraction reactions in the nanocrystalline form vis a vis the bulk form. This is attributed, at least in part, to the ability of nanocrystalline materials to accommodate more strain accompanying Li insertion/extraction reactions and also because they provide short path lengths for Li^+ diffusion.[1] High charge–discharge rates are achieved by using nanocrystalline materials as electrodes for Li-ion batteries. Particle size effects on lithium reactivity are well studied for nanophase transition metal oxides, wherein the lithium is reversibly extracted from Li_2O with concomitant oxidation/reduction of transition metal.[2,3] As far as the classical lithium insertion process is concerned, particle size effect is well demonstrated in the case of α-Fe_2O_3.[4] In the 0.5 μm sized particles of α-Fe_2O_3, $0.1Li/Fe_2O_3$ can be inserted prior to the phase transformation from hcp to ccp, whereas in 20 nm sized particles insertion of $1Li/Fe_2O_3$ is achieved. Following these reports, high reactivity of Li in nanocrystalline rutile TiO_2 [5–8] and mesoporous rutile type MnO_2[9] was shown. Very recently, we have demonstrated the Li intercalation into nanocrystalline brookite type TiO_2,[10] wherein 0.9Li can be intercalated during the initial discharge. In contrast, only 0.1 to 0.2Li can be intercalated into submicrometer sized particles.[11] The remarkable feature of this material is that its structure is stable even after 0.9Li intercalation, and it exhibits a reversible capacity of 170 mA h g^{-1} even after 40 cycles. These studies indicate that all materials hitherto showing low reactivity toward Li intercalation in the bulk form need to be revisited in the nanocrystalline form. Here, we describe another example, $MgTi_2O_5$, wherein we observed a remarkable difference in the material response between micro- and nanometer sized particles toward Li insertion.

$MgTi_2O_5$ crystallizes in the pseudo-brookite structure with space group *Bbmm*.[12,13] The structure is built up of double chains of edge sharing $M(1)O_6$ and $M(2)O_6$ octahedra running along the 'b' direction (Figure 1). These double chains are connected by edges and corners in the ac plane. This arrangement leads to one-dimensional channels along the b direction suggesting the possibility of lithium insertion. Both $M(1)O_6$ and $M(2)O_6$ octahedra are highly distorted. The structural arrangement is such that the $M(1)O_6$ octahedra are larger in size and more distorted than $M(2)O_6$ octahedra. There are four M(1) and eight M(2) sites per unit cell. The distribution of Mg and Ti between the two sites varies depending on the synthesis conditions resulting in slight

* Corresponding author. E-mail: varada@iitm.ac.in. Tel: 91-44-2257 4215. Fax: 91-44-2257 0509.
[†] Indian Institute of Technology Madras.
[‡] CNRS ENSICAEN.

(1) Arico, A. S.; Bruce, P.; Scrosati, B.; Tarascon, J.-M.; Van Schalkwijki, W. *Nat. Mater.* **2005**, *4*, 366.
(2) Poizot, P.; Laruelle, S.; Grugeon, S.; Dupont, L.; Tarascon, J.-M. *Nature* **2000**, *407*, 496.
(3) Tarascon, J.-M; Grugeon, S.; Laruelle, S.; Larcher, D.; Poizot, P. In *Lithium Batteries*; Nazri, G.-A., Pistoia, G., Eds.; Kluwer Academic Publishers: Norwell, 2004; pp 220−246.
(4) Larcher, D.; Masquelier, C.; Bonnin, D.; Chabre, Y.; Masson, V.; Leriche, J.-B.; Tarascon, J.-M. *J. Electrochem. Soc.* **2003**, *150*, A133.
(5) Hu, Y.-S.; Kienle, L.; Guo, Y.-G.; Maier, J. *Adv. Mater.* **2006**, *18*, 1421.
(6) Anji Reddy, M.; Satya Kishore, M.; Pralong, V.; Caignaert, V.; Varadaraju, U. V.; Raveau, B. *Electrochem. Commun.* **2006**, *8*, 1299.
(7) Baudrin, E.; Cassaignon, S.; Koelsch, M.; Jolivet, J.-P.; Dupont, L.; Tarascon, J.-M. *Electrochem. Commun.* **2007**, *9*, 337.
(8) Jiang, C.; Honma, I.; Kudo, T.; Zhou, H. *Electrochem. Solid-State Lett.* **2007**, *10*, A127.
(9) Luo, J. Y.; Zhang, J. J.; Xia, Y. Y. *Chem. Mater.* **2006**, *18*, 5618.
(10) Reddy, M. A.; Kishore, M. S.; Pralong, V.; Varadaraju, U. V.; Raveau, B. *Electrochem. Solid-State Lett.* **2007**, *10*, A29.
(11) Reddy, M. A.; Kishore, M. S.; Pralong, V.; Varadaraju, U. V.; Raveau, B. Manuscript in preparation.
(12) Barry, B.; Wechsler, A.; Von Dreele, R. B. *Acta Crystallogr.* **1989**, *B45*, 542.
(13) Yang, H.; Hazen, R. M. *J. Solid State Chem.* **1998**, *138*, 238.

10.1021/cm7028239 CCC: $40.75
Published on Web 02/27/2008

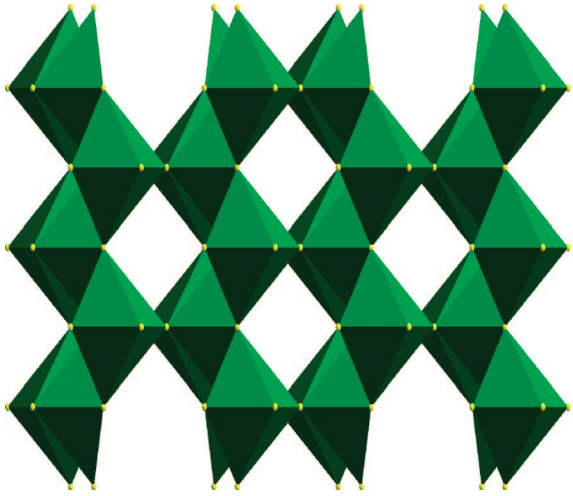

Figure 1. Crystal structure view of $MgTi_2O_5$ in the *ac* plane.

variations in the lattice parameters.[13] In $MgTi_2O_5$, in principle, 2Li can be inserted per formula unit by using the redox couple of Ti^{4+}/Ti^{3+}, leading to a theoretical specific capacity of 266 mA h g^{-1}. The high theoretical specific capacity motivated us to study the lithium insertion behavior in $MgTi_2O_5$.

Conventionally, $MgTi_2O_5$ can be prepared by annealing stoichiometric amounts of MgO and TiO_2 at 1200−1400 °C for long duration resulting in micrometer sized particles.[12] Various low temperature routes were proposed to prepare nanometer sized and/or submicrometer sized samples of $MgTi_2O_5$.[14–16] In all the methods either titanium alkoxides or $TiCl_4$ were used as precursors. However, these titanium salts are highly moisture sensitive, and it is difficult to obtain single phase products due to unwanted side reactions. In the present work, we report the synthesis of nanocrystalline $MgTi_2O_5$ by a convenient polymerizable-complex method.

Experimental Section

Micrometer sized samples of $MgTi_2O_5$ were prepared by solid state reaction method starting from high pure $Mg(CH_3COO)_2 \cdot 4H_2O$ and anatase TiO_2. Stoichiometric amounts of the reactants were ground well and heated in air at 1200 °C for 24 h and quenched to room temperature. Nanometer sized $MgTi_2O_5$ was prepared by Pechini type polymeric precursor method. In a typical synthesis, 0.47 g of titanium metal was dissolved in an ice cold solution containing 40 mL of hydrogen peroxide (30%) and 10 mL of ammonia (28%). To the obtained transparent light yellow colored solution, stoichiometric amounts of citric acid and $Mg(CH_3COO)_2 \cdot 4H_2O$ were added, and the resulting solution was stirred for a few hours at 60 °C to ensure the formation of the metal complex. To this solution was added ethylene glycol, and the temperature was raised to 90 °C for the polyesterfication step to proceed. The metal/citric acid/ethylene glycol ratio was maintained as 1:1:1. A reddish colored viscous gel resulted, which was dried at 120 °C. Further heating of the dried gel at 300 °C resulted in the precursor. A similar method was recently reported for the synthesis of lithium lanthanum titanate.[17] XRD patterns were recorded in the 2θ range 5–120° using a Philips X'pert diffractometer with Bragg–Brentano geometry equipped with Cu Kα radiation. The structure refinement was carried out using the FULLPROF refinement program. Electron diffraction study was carried out on a JEOL 200CX transmission electron microscope (TEM) equipped with a KEVEX analyzer (energy dispersive spectroscopy). A scanning electron microscope (SEM) Philips Field Effect Gun (FEG) XL-30 was used to study the sample morphology. The electrochemical studies were performed in Swagelok type cells. The cells were assembled in an argon filled glovebox. Lithium metal was used as the negative electrode, and a borosilicate glass fiber sheet (separator) was saturated with 1 M $LiPF_6$ in 1:1 ethylene carbonate (EC)/dimethyl carbonate (DMC) (LP30, Merck) electrolyte. Electrodes were fabricated by mixing active material, acetylene black (Denka Singapore Pvt. Ltd.), and poly(vinylidene fluoride) (PVDF) in the weight ratios 70:20:10. A slurry containing the above mixture was prepared by using *N*-methyl-2-pyrrolidinone and was spread on a stainless steel (s.s.) foil (1.4 cm diameter; area ∼ 1.5 cm^2) and dried in an oven at 100 °C for 12 h. The electrochemical studies were carried out at RT using a VMP II potentiostat/galvanostat (Biologic SA, Claix, France) or by using Arbin battery cycling unit. In a typical experiment, 5 mg of the active material is taken, and a constant current of 14 mA g^{-1} (∼C/10 rate) was passed. This corresponds to a current density of 10 mA/cm^2. Ex situ XRD patterns were recorded on the electrodes under vacuum by using a special chamber attached to the XRD instrument.

Table 1. Refined Lattice Parameters and Site Occupancies of Bulk and Nano-$MgTi_2O_5$

parameter	$MgTi_2O_5$ synthesized by solid state method	$MgTi_2O_5$ synthesized by sol–gel method
a, Å	9.7490(4)	9.759(9)
b, Å	9.9908(4)	10.003(9)
c, Å	3.7456(2)	3.740(3)
χ^2, Rf, Bragg R-factor	8.41, 6.42, 4.75	4.13, 7.42, 8.17
occupancy M(1) site Mg(1)/Ti(1)	0.64(1)/0.36(1)	0.34(2)/0.66(2)
occupancy M(2) site Mg(2)/Ti(2)	0.18(1)/0.82(1)	0.33(2)/0.67(2)

Results and Discussion

In the course of solid-state reaction starting from $Mg(CH_3COO)_2 \cdot 4H_2O$ and TiO_2, single phase $MgTi_2O_5$ was obtained when the reaction was carried out at 1200 °C. If the reaction was carried out at temperatures less than 1200 °C, ilmenite $MgTiO_3$ and TiO_2 were always present as impurities. The PXRD pattern is refined on the basis of the orthorhombic cell (space group *Bbmm*), and the lattice parameters are $a = 9.7490(4)$ Å, $b = 9.9908(4)$ Å, and $c = 3.7456(2)$ Å. The occupancies of Mg/Ti in the M(1) and M(2) sites are given in Table 1. SEM analysis shows agglomeration of the particles. The particle size is in the range 2–5 μm (see Supporting Information).

To obtain nanometer sized particles of $MgTi_2O_5$, the polymerizable-complex (PC) method, also known as the "Pechini method" was adopted.[18] This method is based on metal complex formation followed by polyesterification using polyhydroxy alcohol. The arresting of the metal complex in

(14) Pfaff, G. *Ceram. Int.* **1994**, *20*, 111.
(15) Purohit, R. D.; Saha, S. *Ceram. Int.* **1999**, *25*, 475.
(16) Bokhimi, X.; Boldú, J. L.; Munoz, E.; Novaro, O.; López, T.; Hernández, J.; Gómez, R.; García-Ruiz, A. *Chem. Mater.* **1999**, *11*, 2716.
(17) Vijayakumar, M.; Inaguma, Y.; Mashiko, W.; Crosnier-Lopez, M.-P.; Bohnke, C. *Chem. Mater.* **2004**, *16*, 2719.
(18) Pechini, M. P. U.S. Patent 3,330,697, 1967.

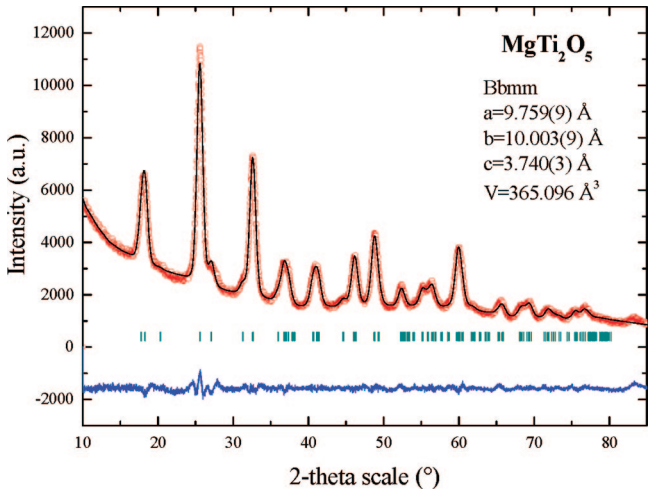

Figure 2. Rietveld refined PXRD pattern of $MgTi_2O_5$ synthesized by the PC method.

a polymer network prevents segregation of metal ions, thereby ensuring compositional homogeneity. Calcination of polymeric precursor at moderate temperatures yields pure metal oxides. The key step in the PC method is the preparation of highly water soluble metal complexes. In the present study, water soluble titanium citrate complex was prepared following the method suggested by Kakihana et al.[19] The detailed procedure to obtain the polymeric gel and the precursor is given in the experimental section. The obtained precursor was ground well and calcined at 500 °C for 2 h in air. The resulting powder was black in color indicating the incomplete decomposition of the organic moieties. Moreover, it is amorphous as revealed by XRD analysis. By increasing the calcination temperature to 600 °C for 2 h, single phase $MgTi_2O_5$ was obtained. However, further increase in calcination time or temperature leads to the formation of an impurity phase, $MgTiO_3$. Thus, the temperature and time of heating are critical to obtain phase pure $MgTi_2O_5$. In comparison, in the solid state reaction between $Mg(CH_3COO)_2 \cdot 4H_2O$ and TiO_2 at 600 °C, only $MgTiO_3$ is formed. The Rietveld refined PXRD profile of $MgTi_2O_5$ synthesized by PC method at 600 °C is shown in Figure 2. The calculated lattice parameters are $a = 9.759(9)$ Å, $b = 10.003(9)$ Å, and $c = 3.740(3)$ Å. The occupancies of Mg/Ti in the M(1) and M(2) sites are given in Table 1. It is evident that the occupancies are different in the sol–gel derived sample (nanophase) vis a vis sample synthesized by high temperature solid state reaction (bulk). The mean crystallite size calculated from the XRD pattern using the Scherrer's formula is ~9 nm. The TEM image (Figure 3a) of $MgTi_2O_5$ shows that the sample is composed of aggregated nanocrystallites. The selected area electron diffraction (SAED; Figure 3b) shows the ring pattern, revealing the nanocrystalline nature of the sample. From the HRTEM image (Figure 3c) it can be seen that the crystallite size is of the order of 10 nm, consistent with the value obtained from the XRD data.

Figure 4a shows the voltage−composition profiles of micrometer sized $MgTi_2O_5$ in the voltage window 0.5–3.0 V at C/10 rate. Two plateaus are evident (reflected as peaks in the differential capacity plot in the inset of Figure 4a). The plateau at 1.1 V corresponds to lithium insertion into $MgTi_2O_5$ and is indicative of biphasic nature of the insertion reaction. The low voltage plateau (0.7 V) can be due to the reaction of Li with acetylene black. After subtraction of the capacity due to acetylene black, the initial discharge capacity corresponds to insertion of 0.7Li into $MgTi_2O_5$. During the initial charge, there is a large irreversible capacity loss, and a negligible amount of Li is extracted (~0.1Li). We have carried out lithium insertion studies on the micrometer sized $MgTi_2O_5$ using 1.6 M *n*-butyl lithium in hexane (stirred at RT for 3 days). We did not observe any significant lithium insertion. The reason for this could be that the potential of *n*-butyl lithium is equivalent to 1 V versus Li, and from the discharge curves of the micrometer sized $MgTi_2O_5$ (Figure 4a) it is evident that the first intercalation occurs at approximately 1.1 V. When we carried out chemical lithiation using *n*-butyl lithium at 50 °C, we did observe some insertion (~0.3Li) in micrometer sized $MgTi_2O_5$.

To understand the structural changes accompanying Li insertion, we recorded the ex situ XRD pattern on the completely discharged electrode. Figure 4b compares the XRD patterns of micrometer sized $MgTi_2O_5$ (i) before and (ii) after Li insertion. It is evident that the initial structure is retained after Li insertion. The refinement of pattern (ii) indicates the presence of two phases, namely, parent $MgTi_2O_5$ and the lithiated phase. This corroborates well with the presence of a plateau in the voltage−composition profile. The XRD pattern of the lithiated phase can be indexed on the basis of the same space group as that of the parent phase (*Bbmm*) with the orthorhombic lattice parameters $a = 9.7082(6)$ Å, $b = 9.9399(5)$ Å, and $c = 3.8283$ (3) Å. Thus, upon lithium insertion, there is a decrease in "*a*" and "*b*" lattice parameters, whereas the "*c*" parameter increases with a marginal increase in the volume of the unit cell. This suggests that there is an anisotropic displacement of metal and/or oxygen atoms in the lattice to accommodate the inserted lithium. Grey et al. studied the nonstoichiometric Li-pseudo-brookite in the $Li_2O-Fe_2O_3-TiO_2$ system and found deviation from the stoichiometric Fe_2TiO_5 with composition, $Li_{0.81}Fe_{0.27}Ti_{2.09}O_5$ ($M_{3.17}O_5$).[20] They refined the structure of $Li_{0.81}Fe_{0.27}Ti_{2.09}O_5$ using neutron diffraction and concluded that the excess Li (0.17) occupies a five coordinated (w.r.t. oxygen) interstitial site with square pyramidal geometry. Thus, in the present study, it is rational to assume that the inserted Li in $MgTi_2O_5$ occupies interstitial square pyramidal sites which share faces with $M(1)O_6$ octahedra. Despite the structural stability toward Li insertion, no reversibility was observed. The low reactivity and irreversibility of micrometer sized $MgTi_2O_5$ prompted us to study the nanocrystalline form.

Figure 5a shows the variation of cell voltage versus composition of nanometer sized $MgTi_2O_5$. The charge/discharge curves were obtained by passing a constant current of 14 mA g^{-1} (~C/10 rate; reaction of 1Li in 10 h) in the

(19) Kakihana, M.; Tada, M.; Shiro, M.; Petrykin, V.; Osadam, M.; Nakamura, Y. *Inorg. Chem.* **2001**, *40*, 891.

(20) Grey, I. E.; Li, C.; Ness, T. *J. Solid State Chem.* **1998**, *141*, 221.

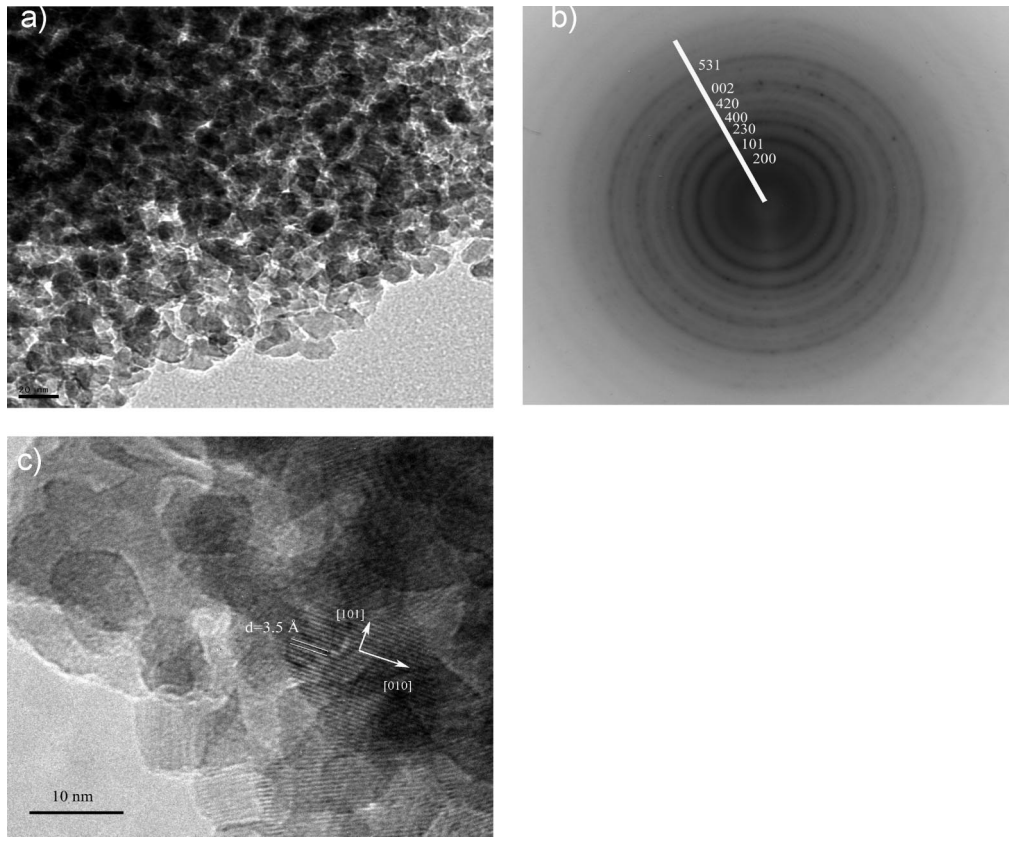

Figure 3. (a) TEM micrograph of $MgTi_2O_5$ synthesized by the PC method, (b) corresponding SAED pattern, and (c) HRTEM image.

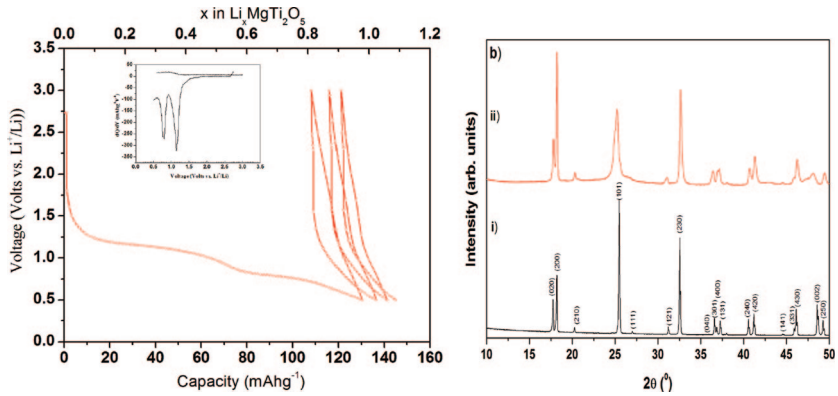

Figure 4. (a) Voltage−composition profiles of micrometer sized $MgTi_2O_5$ (inset shows differential capacity plot); (b) ex situ XRD patterns of micrometer $MgTi_2O_5$ (i) before and (ii) after lithium insertion.

voltage window 1.0–3.0 V. The behavior of the nanosized $MgTi_2O_5$ is different from that of the microsized material. Initially, the voltage drops sharply to 2.2 V (from OCV). Subsequently the voltage decreases monotonously to 1.3 V. About 0.6Li are inserted in this voltage window. The monotonous decrease in voltage (absence of plateau) indicates a solid solution regime. This behavior is in contrast to that of microsized $MgTi_2O_5$, wherein the insertion of about 0.7Li is a biphasic reaction (plateau). On further discharge, a plateau-like behavior is observed, and 1.5Li are inserted at almost a constant voltage of 1.1 V.

The inset in Figure 5a shows a peak in the differential capacity plot corresponding to the plateau in the first discharge. A total of 2.1Li are inserted, leading to a capacity of 281 mA h g^{-1}. During the first charge, 1.3Li are extracted with large polarization between charge and discharge. Thus, in the first charge lithium is not completely extracted, and 0.8Li are retained in the structure. The differential capacity plot (inset in Figure 5a) indicates two processes in the charge curve, the origin of which is unknown at present. The two plateaus are seen in the subsequent charge/discharge curves (not shown) even after 10 cycles. When, instead of discharging the cell to 1.0 V, only 1Li is inserted into the structure, very poor reversibility is observed. This clearly suggests that the lithium that is inserted into the structure during the initial stages of discharge is not reversible. This is in line with the observation of irreversibility in the case of the micrometer sized sample. The cycling behavior of nanosized $MgTi_2O_5$ is presented in Figure 5b. During cycling, the capacity fades gradually and reaches a value of 130 mA h g^{-1} (∼1Li), which is stable even after 50 cycles.

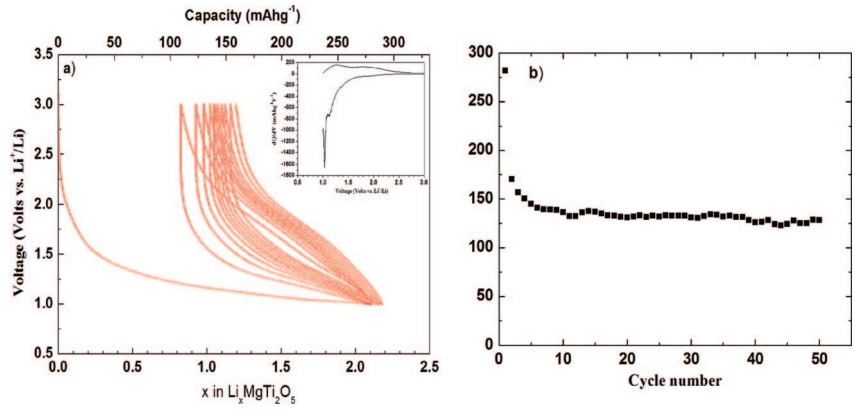

Figure 5. (a) Voltage−composition profiles of nanometer sized $MgTi_2O_5$ (inset shows differential capacity plot); (b) cycling behavior of the nanometer sized $MgTi_2O_5$.

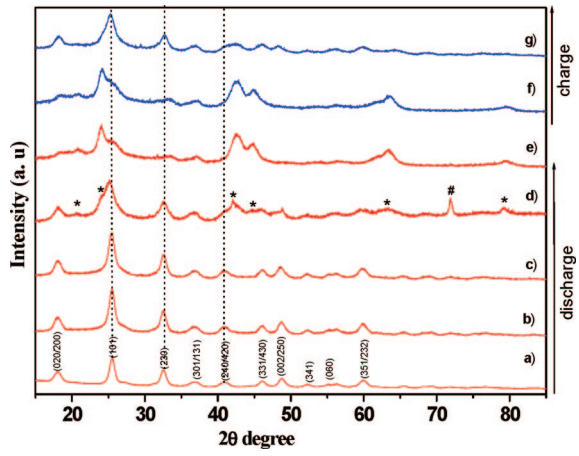

Figure 6. Ex situ XRD pattern nanosized $MgTi_2O_5$ during discharge (a) $MgTi_2O_5$, (b) $Li_{0.5}MgTi_2O_5$, (c) $LiMgTi_2O_5$, (d) $Li_{1.5}MgTi_2O_5$, and (e) $Li_2MgTi_2O_5$ and during charge (f) $Li_{1.5}MgTi_2O_5$ and (g) $Li_{0.7}MgTi_2O_5$.

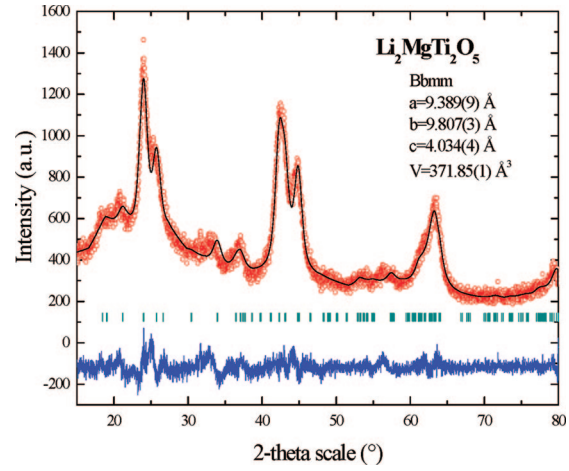

Figure 7. Profile fitted (pattern matching) PXRD pattern of nanometer sized $Li_2MgTi_2O_5$.

To understand the structural changes associated with Li insertion, ex situ XRD patterns of the electrodes after every insertion/extraction of 0.5Li are recorded (Figure 6). The compositions are nominal and it is assumed that all the Li reacted is inserted into $MgTi_2O_5$. During the insertion of 1Li, corresponding to the composition $LiMgTi_2O_5$, there are no prominent changes in the XRD pattern of $MgTi_2O_5$. It is possible that there may be a small shift in the peak positions as observed in the case of micrometer sized sample. However, since the peaks are broad in the nanocrystalline phase, any minor changes in the peak positions may not be readily discernible. Further insertion of 0.5Li brings about significant changes in the XRD pattern. A few new peaks are seen which are marked by "*" in Figure 6d. As the extent of Li insertion increases from 1.5 to 2Li, the intensity of the newly evolved peaks increases and the peaks corresponding to $LiMgTi_2O_5$ disappear. During the extraction of lithium, the peaks corresponding to $LiMgTi_2O_5$ are recovered at the expense of the newly evolved peaks.

Figure 7 shows the profile fitted (pattern matching) PXRD pattern of $Li_2MgTi_2O_5$. We have attempted Rietveld refinement of the lithiated phases. However, we are unable to arrive at an unequivocal solution because of the broadness of the peaks caused by the RT intercalation reaction. The diffraction peaks of the parent phase themselves are broad due to the nanophase nature of the materials, and the problem is further compounded by the RT intercalation reaction. This limits our understanding of the causes of structural origin, including possible Mg^{2+} ion migration upon Li intercalation, in determining the ICL and the "two plateau" behavior. The peaks could be indexed on the basis of the same space group as that of the parent phase (*Bbmm*). The lattice parameters are $a = 9.389$ (9) Å, $b = 9.807(3)$ Å, and $c = 4.034$ (4) Å. Figure 8a,b shows the HRTEM image of the $Li_2MgTi_2O_5$ and the corresponding electron diffraction, respectively. HRTEM shows the presence of nanocrystallites characterized by lattice fringes. The lattice fringes are found to be 4.9 Å and 3.5 Å (spots 1 and 2 on the FFT spectrum), which could correspond to the (020) and (111) planes of the pseudo-brookite type phase. In addition, the measured interplanar angle of the two sets of fringes is 70.7° in accordance with the calculated angle between these two planes. Spot 3 on the FFT spectra could also be indexed as the (020) interplanar distance.

The spot 4 of the FFT (from another particle) reveals interplanar distance of 3.7 Å, which corresponds to the (101) plane. Thus, from the HRTEM analysis, it can be concluded that the structure of the fully lithiated phase is akin to that of the parent phase and that all the reflections could be indexed based on the same space group as that of the parent phase, namely, *Bbmm*. The SAED pattern shows rings that are ascribed to the four main lines observed in the XRD

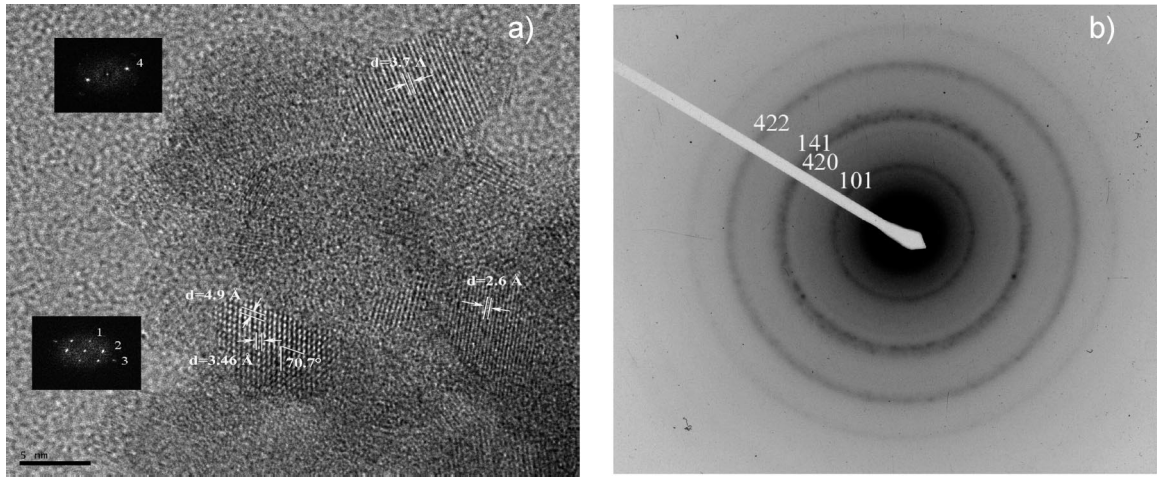

Figure 8. HRTEM image of (a) $Li_2MgTi_2O_5$ and (b) corresponding SAED pattern.

pattern, namely, (101), (420), (141), and (422). This confirms that the structural integrity is retained even after 2Li are inserted into the lattice of $MgTi_2O_5$ in the nanophase, underlining the importance of the nanocrystalline state in augmenting the stability of the structure toward Li insertion/deinsertion reactions. The large family of phases crystallizing in the pseudo-brookite structure, thus, provides a unique opportunity to understand the importance of the nanocrystalline state in determining the Li insertion behavior, and studies are currently underway on other phases with pseudo-brookite structure.

Conclusion

In conclusion, we have successfully synthesized nanocrystalline $MgTi_2O_5$ by polymerizable precursor method. We observe high reactivity of nanocrystalline $MgTi_2O_5$ towards lithium vis a vis the bulk form. 2Li can be inserted into nanocrystalline $MgTi_2O_5$ of which 1Li is reversible ($Li_2MgTi_2O_5 \leftrightarrow LiMgTi_2O_5$) giving a specific capacity of 130 mA h g^{-1} in the voltage window 1.0–3.0 V at C/10 rate. On the other hand, in micrometer sized particles, only about 0.8 Li are irreversibly inserted. Because nanosized materials are capable of accommodating strain accompanying insertion reactions more than the bulk materials, the insertion of 2Li per formula unit in nanosized $MgTi_2O_5$ can be rationalized. This study amply demonstrates the importance of nanocrystalline materials in facilitating the Li insertion reactions and therefore in the design of electrode materials for Li-ion batteries.

Acknowledgment. This work is carried out in the framework of LAFICS, and the financial support from IFCPAR (Indo-French Centre for the Promotion of Advanced Research/Centre Franco-Indien Pour la Promotion de la Recherche Avancee) is gratefully acknowledged. V.P. thanks M. Hervieu and P. Boullay for their help in TEM studies.

Supporting Information Available: Phase evolution of $MgTi_2O_5$ during solid state and sol–gel synthesis, Rietveld refined powder XRD pattern of micrometer sized $MgTi_2O_5$, and SEM analysis (PDF). This material is available free of charge via the Internet at http://pubs.acs.org.

CM7028239